Preplanned Studies

# A Retrospective Modeling Study of the Targeted Non-Pharmaceutical Interventions During the Xinfadi Outbreak in the Early Stage of the COVID-19 Pandemic — Beijing, China, 2020

Yan Wang[1,&]; Kaiyuan Sun[2,&]; Yang Pan[3,&]; Lan Yi[4]; Da Huo[3]; Yanpeng Wu[4]; Shuaibing Dong[3]; Jinxin Guo[1]; Xiangfeng Dou[3]; Wei Wang[1]; Shuangsheng Wu[3]; Xufang Bai[1]; Hongjie Yu[1,4,#]; Quanyi Wang[3,#]

**Summary**

**What is already known about this topic?**

China has repeatedly contained multiple severe acute respiratory syndrome coronavirus 2 (SARS-CoV-2) outbreaks through a comprehensive set of targeted non-pharmaceutical interventions (NPIs). However, the effectiveness of such NPIs has not been systematically assessed.

**What is added by this report?**

A multilayer deployment of case isolation, contact tracing, targeted community lockdowns, and mobility restrictions could potentially contain outbreaks caused by the SARS-CoV-2 ancestral strain, without the requirement of city-wide lockdowns. Mass testing could further aid in the efficacy and speed of containment.

**What are the implications for public health practice?**

Pursuing containment in a timely fashion at the beginning of the pandemic, before the virus had the opportunity to spread and undergo extensive adaptive evolution, could help in averting an overall pandemic disease burden and be socioeconomically cost-effective.

Three years into the coronavirus disease 2019 (COVID-19) pandemic, several severe acute respiratory syndrome coronavirus 2 (SARS-CoV-2) variants have emerged with increasing potency in the human population, causing considerable morbidity and mortality worldwide, while Chinese mainland had been able to maintain local containment through an extensive set of targeted non-pharmaceutical interventions (NPIs) (*1*). Here we developed a fully stochastic, spatially structured, agent-based model of SARS-CoV-2 ancestral strain and reconstructed the Beijing Xinfadi outbreak between June 11 and July 10, 2020. This quantitatively assessed the feasibility and prerequisites for containing the virus before it had the opportunity to acquire its highly transmissivity and immune-evasive properties. We found that screening for symptoms and among high-risk populations served as an aid in uncovering the cryptic community transmission in the early stages of the outbreak. Effective contact tracing greatly reduces transmission. Targeted community lockdowns and temporal mobility restrictions could slow down the spatial spread of the virus. Mass testing could further improve the speed at which the outbreak is contained. Our analysis suggests that the containment of SARS-CoV-2 ancestral strains was certainly feasible. Early in time measures to stop further spread of the outbreak, prevent mutation of the virus into a more deadly variant is cost-effective and can save lives.

The Beijing Xinfadi Wholesale Market outbreak was initially identified on June 11, 2020, shortly after the successful suppression of the initial wave in Wuhan that ended in March 2020 and caused by the ancestral strain of SARS-CoV-2, with the D614G mutation reintroduced from outside China (*2*). Other details of the outbreak have been previously described (*3*–*5*). It is ideal to imitate a generic model of initial containment for countries other than China following the emergence and exportation of SARS-CoV-2 ancestral strain, as few adaptive mutations had been acquired and the herd immunity was negligible (no available vaccine and few prior SARS-CoV-2 infections) during the outbreak. The timing gap between the initial and the Xinfadi Wholesale Market outbreaks also allowed Beijing to expand its SARS-CoV-2 molecular testing capacity (with an initial testing capacity of 100,000 tests per day ramped up to 500,000 tests per day by July 7, 2020), permitting mass testing of the population at risk.

We first analyzed the highly detailed line-list data of the outbreak that had been extracted from the

Notifiable Infectious Disease Reporting System and the Epidemiological Investigation Information System of the People's Republic of China to characterize the epidemiological patterns of the outbreak. We then developed a fully stochastic, spatially structured agent-based model to reconstruct the containment effort and recover the epidemiologic patterns observed in the epidemiological data. The model structure, detailed in the Supplementary Material and Supplementary Tables S1–S5 (available in https://weekly.chinacdc.cn/), was well informed by high-resolution population mobility data, allowing us to explicitly model the targeted testing and intervention programme at high spatial resolution. Lastly, we created eight possible intervention scenarios (Levels 1–8, Table 1) by progressively layering additional NPIs on top of the prior scenario, to dissect the relative contribution of each intervention individually to the overall containment of the Xinfadi outbreak.

We ran 500 simulations with each scenario capturing the stochasticity of the transmission process. For each simulation, the following summary statistics were calculated to quantify the impact of each intervention individually: 1) the overall effective reproduction number ($R_{eff}$), defined as the average of the individual reproduction number of each individual infected after the implementation of NPIs; 2) the total number of infections ($N$) before July 10, 2020 (the end date of the Xinfadi outbreak); and 3) the proportion of undetected infections. The details of each NPI in

TABLE 1. Hypothetical intervention parameters of each NPI in different simulation scenarios.

| NPI | Level 1 | Level 2 | Level 3 | Level 4 | Level 5 | Level 6 | Level 7 | Level 8 |
|---|---|---|---|---|---|---|---|---|
| Symptom surveillance | | | | | | | | |
| Percentage of detected symptomatic infections (%) | 66.7 | 66.7 | 66.7 | 66.7 | 66.7 | 66.7 | 66.7 | 66.7 |
| Mask wearing | | | | | | | | |
| Percentage of population wearing masks in the workplace (%) | – | 20 | 20 | 20 | 20 | 20 | 20 | 20 |
| Percentage of population wearing masks in the community (%) | – | 50 | 50 | 50 | 50 | 50 | 50 | 50 |
| Closure of the Xinfadi Wholesale Market | | | | | | | | |
| Date of closure | – | – | 2020-06-13 | 2020-06-13 | 2020-06-13 | 2020-06-13 | 2020-06-13 | 2020-06-13 |
| Quarantine of key population | | | | | | | | |
| Workers at the Xinfadi Wholesale Market | – | – | – | Centralized | Centralized | Centralized | Centralized | Centralized |
| Visitors to the Xinfadi Wholesale Market | – | – | – | Home | Home | Home | Home | Home |
| Residents around the Xinfadi Wholesale Market | – | – | – | Lockdown | Lockdown | Lockdown | Lockdown | Lockdown |
| Contact tracing | | | | | | | | |
| Percentage of traced household contact (%) | – | – | – | – | 100 | 100 | 100 | 100 |
| Percentage of traced work contact (%) | – | – | – | – | 100 | 100 | 100 | 100 |
| Percentage of traced community contact (%) | – | – | – | – | 70 | 70 | 70 | 70 |
| Residential community lockdown | | | | | | | | |
| Duration of lockdown after the identification of the last case (days) | – | – | – | – | – | 14 | 14 | 14 |
| Mobility restrictions* | | | | | | | | |
| Percentage of mobility reductions in high-risk region (%) | – | – | – | – | – | – | 70 | 70 |
| Percentage of mobility reductions in moderate-risk region (%) | – | – | – | – | – | – | 50 | 50 |
| Percentage of mobility reductions in low-risk region (%) | – | – | – | – | – | – | 20 | 20 |
| Mass testing | | | | | | | | |
| Rounds of RT-PCR testing | – | – | – | – | – | – | – | 3 |

Note: "–" means not applicable.
Abbreviation: NPI=non-pharmaceutical intervention; RT-PCR=reverse transcription-polymerase chain reaction.
* The intervention parameters of mobility restrictions are defined as percentages of reductions in population flows between different risk regions during the Xinfadi outbreak, detailed in the Supplementary Table S5 (available in https://weekly.chinacdc.cn/).

response to the Xinfadi outbreak were described in the Supplementary Materials. The model was coded in Python (version 3.10.4, Python Software Foundation, Fredericksburg, VA, US). The statistical analyses and visualization were performed using R (version 4.0.2, R Foundation, Vienna, Austria).

A total of 368 SARS-CoV-2 infections were reported during the Xinfadi outbreak, including 335 (91.03%) confirmed cases and 33 (8.97%) asymptomatic infections (Figure 1A). Most of the infections were clustered in or around Huaxiang Street, where the Xinfadi Wholesale Market was located (Figure 1B), and were aged between 20 and 59 years (Figure 1C). Simulations closely the imitate real world. We present one realization of the temporal distributions of the reported infections (Figure 1D). Similar to the observed distribution in Figure 1A, a total of 355 infections were detected in the simulated outbreak, of which 18.87% were asymptomatic infections and 81.13% were confirmed cases. Figure 1E–F show the spatial distribution and age profile of the infections aggregating from the results of 500 simulated outbreaks. Both the spatial patterns and age distributions were similar to the real-world observations in Figure 1B–C, with most of the infections detected around the Xinfadi Wholesale Market and in the working age population.

To quantify the relative contribution of each individual NPI to outbreak containment, we consecutively added each intervention to the unmitigated chains of transmission. The estimated effective reproduction numbers ($R_{eff}$) and total number of infections ($N$) are reported in Figure 2A and Figure 2B. We found heterogeneity across simulations even under the same intervention intensity, reflecting the intrinsic stochasticity of SARS-CoV-2 transmission. We found that the outbreak could not be contained with only symptom surveillance (Level 1) due to the pre-symptomatic and asymptomatic transmission of SARS-CoV-2, with a median $R_{eff}$ = 2.05 and a median $N$=13,421, respectively. Layering mask wearing (Level 2) and closure of Xinfadi Wholesale Market (Level 3) did not lead to significant improvement, with all simulations having effective reproduction numbers larger than 1.8, well above the epidemic threshold. Quarantine of the key populations (Level 4) could remove the potential infections from the susceptible population at the early phase of viral

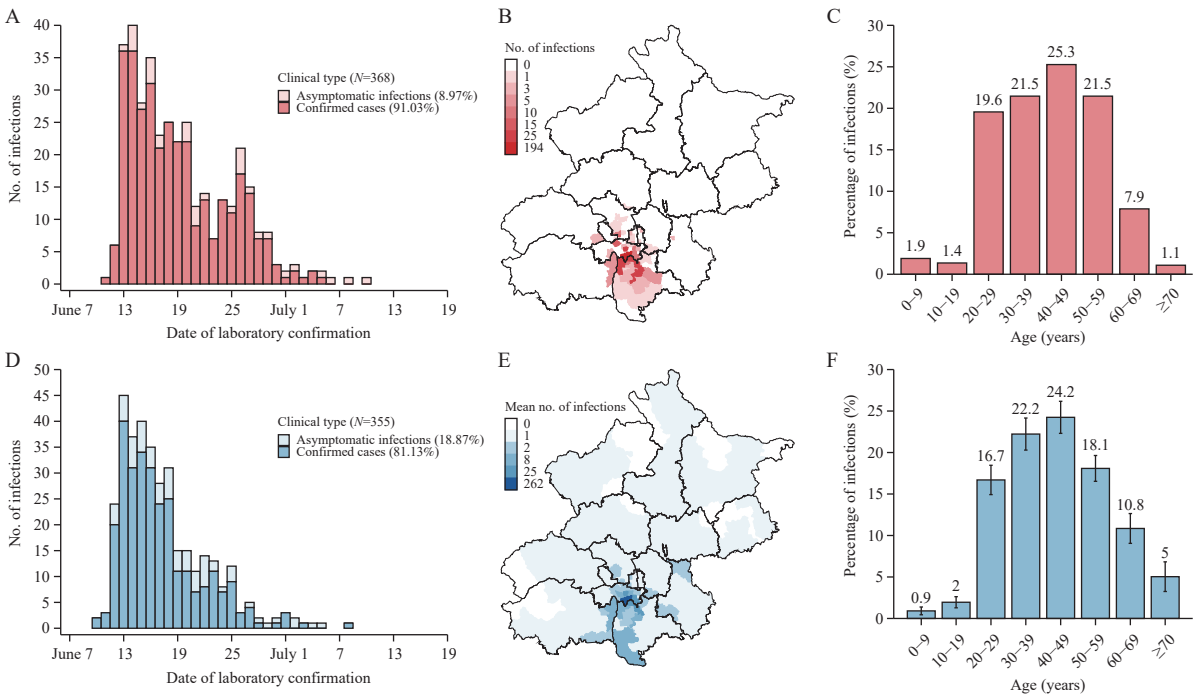


FIGURE 1. Observed and simulated epidemiologic patterns during the Xinfadi outbreak. (A) Observed temporal distribution of SARS-CoV-2 infections stratified by clinical type. (B) Observed spatial distribution of SARS-CoV-2 infections. (C) Observed age distribution of SARS-CoV-2 infections. (D) Time series of SARS-CoV-2 infections stratified by clinical type based on one simulated outbreak. (E) Spatial distribution of SARS-CoV-2 infections estimated based on 500 simulations. (F) Age distribution of SARS-CoV-2 infections estimated based on 500 simulations.
Abbreviation: SARS-CoV-2=severe acute respiratory syndrome coronavirus 2.

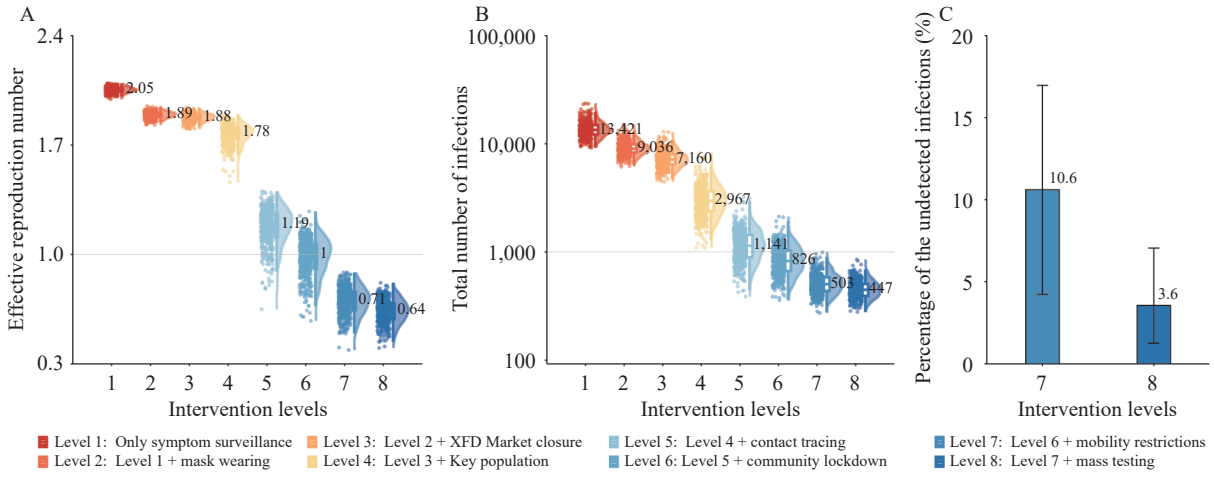


FIGURE 2. The impact of each NPI. (A) Effective reproduction numbers under different intervention scenarios. (B) Number of infections under different intervention scenarios. (C) Proportion of undetected infections.
Note: The bars represent the median of 500 simulations, and the lines give the range of the 2.5 and 97.5 quantiles.
Abbreviation: NPI=non-pharmaceutical intervention, XFD Market=Xinfadi Wholesale Market.

shedding, thus effectively reducing the number of infections (median $N$=2,967), but the further transmission could not be suppressed (median $R_{eff}$ = 1.78). Contact tracing (Level 5), in contrast, could significantly reduce further transmission, leading to fewer infections (median $N$=1,141) and lower effective reproduction numbers (median $R_{eff}$ = 1.19), but for most simulations, the estimated $R_{eff}$ was still above the epidemic threshold, indicating that containment could not be achieved through Level 5 intervention intensity. With lockdown of infected individuals' residential communities (Level 6), the median $R_{eff}$ hovered around the epidemic threshold of 1, resulting in highly stochastic outcomes with the probability of achieving containment at 50%. Implementing targeted population mobility restrictions (Level 7) would achieve the goal of containment, with the estimated $R_{eff}$ ranging from 0.39 to 0.89 and the number of infections less than 1,000 for all simulations. Although the outbreak could be suppressed with Level 7 intervention intensity, additional mass testing at the street/town level was adopted during the Xinfadi outbreak, which could further reduce the effective reproduction number and the number of infections, with a median $R_{eff}$ = 0.64 and a median $N$=447, leading to faster clearance and fewer infections. Furthermore, we found that approximately 10.6% of the infections were undetected in the absence of mass testing (Level 7), while the number of undetected infections fell to 3.6% after the implementation of mass testing (Level 8), indicating that the outbreak could be contained earlier through mass testing, with more infections being detected and isolated, and thus the onward transmission could be truncated (Figure 2C).

## DISCUSSION

In this study, we demonstrated through both empirical data and modeling analysis that a multilayer deployment of targeted NPIs could easily contain outbreaks caused by the SARS-CoV-2 ancestral strain. We found that robust implementation of symptom surveillance and high-risk population screening served as sentinels to discover cryptic community transmission in the early stage of the outbreak. Effective contact tracing combined with case isolation and close contact quarantine have been shown to substantially reduce transmission, highlighting the importance of training and maintaining epidemiologic teams with field experience. Targeted community lockdown and rapid turnaround of molecular testing for the confined population could further limit undetected infections missed by contact tracing, as the transmission of SARS-CoV-2 demonstrates clear spatial clustering. It is more cost-effective than population-wide lockdowns, with fewer people being affected. Temporal reductions in mobility (rather than blanket lockdowns) in and out of regions with high infection risk could slow down the spatial dissemination of the outbreak. If conditions permit, population-wide mass testing could further improve the speed of outbreak containment. These evidences carried critical policy implications for the ongoing COVID-19 pandemic and other epidemics caused by

newly emerged pathogens.

Currently, the adaptive evolution of SARS-CoV-2 continues with no sign of slowing down, with multiple sublineages of SARS-CoV-2 Omicron emerging continuously and causing recurring Omicron waves despite high levels of population immunity achieved by vaccination and natural infection. In addition, unmitigated spreading could also lead to spillover into other animal reservoirs (*6*), leaving pathogen eradication impossible to achieve. In contrast, at the beginning of the pandemic, even with negligible population immunity (i.e., no effective vaccine available), due to the limited transmissibility of the ancestral strain ($R_0$=2.5) (*7*), multiple regions across all socioeconomic statuses successfully achieved temporal suppression of SARS-CoV-2 in the early stage of the pandemic through the implementation of NPIs. In retrospect, had the virus been successfully contained in the early stage of the pandemic, a great deal of the global morbidity, mortality and tremendous socioeconomic costs could have been avoided.

This study was subject to some limitations. First, it suffers from the uncertainty of epidemiological parameters from previous estimates, such as the distribution of the generation interval and the age-specific asymptomatic rates. Second, the temporal span of our simulations is limited. Finally, we cannot simulate all the NPIs during the Xinfadi outbreak, such as the population screening based on the positive environmental samples.

Our study clearly demonstrated that the containment of the SARS-CoV-2 ancestral strain would have been achievable through NPIs once a reliable and scalable diagnostic test became available. More broadly, the critical opportunity window for containing a newly emerged pathogen is in the very early stage of the pandemic, before the pathogen has the opportunity to evolve and adapt in the human population with greatly enhanced transmissibility and immune evasion properties, if all countries decide to pursue such strategies collectively. Furthermore, sustaining SARS-CoV-2 local containment at the early stage of the pandemic could buy some time to achieve high immunization coverage as well as stockpile effective antiviral drugs, potentially ensuring a smooth transition to mitigation strategies while minimizing the overall disease burden.

**Conflicts of interest**: The findings and conclusions in this study are those of the authors and do not necessarily represent the official position of the funding agencies, the National Institutes of Health, or the U.S. Department of Health and Human Services.

**Funding:** Supported by grants from the Key Program of the National Natural Science Foundation of China (82130093) and Shanghai Municipal Science and Technology Major Project (ZD2021CY001).

**doi:** 10.46234/ccdcw2023.020

[#] Corresponding authors: Hongjie Yu, yhj@fudan.edu.cn; Quanyi Wang, wangqy@bjcdc.org.

[1] School of Public Health, Fudan University, Key Laboratory of Public Health Safety, Ministry of Education, Shanghai Municipality, China; [2] Division of International Epidemiology and Population Studies, Fogarty International Center, National Institutes of Health, Bethesda, MD, USA; [3] Beijing Center for Disease Prevention and Control, Beijing Municipality, China; [4] Shanghai Institute of Infectious Disease and Biosecurity, Fudan University, Shanghai Municipality, China.
[&] Joint first authors.

Submitted: November 13, 2022; Accepted: January 09, 2023

## REFERENCES

1. World Health Organization. WHO coronavirus (COVID-19) dashboard. 2022. https://covid19.who.int/. [2022-8-6].
2. Pang XH, Ren LL, Wu SS, Ma WT, Yang J, Di L, et al. Cold-chain food contamination as the possible origin of COVID-19 resurgence in Beijing. Natl Sci Rev 2020;7(12):1861 – 4. http://dx.doi.org/10.1093/nsr/nwaa264.
3. Wang XL, Lin X, Yang P, Wu ZY, Li G, McGoogan JM, et al. Coronavirus disease 2019 outbreak in Beijing's Xinfadi Market, China: a modeling study to inform future resurgence response. Infect Dis Poverty 2021;10(1):62. http://dx.doi.org/10.1186/s40249-021-00843-2.
4. Wu ZY, Wang QY, Zhao J, Yang P, McGoogan JM, Feng ZJ, et al. Time course of a second outbreak of COVID-19 in Beijing, China, June-July 2020. JAMA 2020;324(14):1458 – 9. http://dx.doi.org/10.1001/jama.2020.15894.
5. Wenjie Tan, Peihua Niu, Xiang Zhao, Yang Pan, Yong Zhang, Lijuan Chen, et al. Reemergent Cases of COVID-19 — Xinfadi Wholesales Market, Beijing Municipality, China, June 11, 2020. China CDC Weekly 2020;2(27):502 – 4. http://dx.doi.org/10.46234/ccdcw2020.132.
6. Yen HL, Sit THC, Brackman CJ, Chuk SSY, Gu HG, Tam KWS, et al. Transmission of SARS-CoV-2 delta variant (AY. 127) from pet hamsters to humans, leading to onward human-to-human transmission: a case study. Lancet 2022;399(10329):1070 – 8. http://dx.doi.org/10.1016/s0140-6736(22)00326-9.
7. Imai N, Cori A, Dorigatti I, Baguelin M, Donnelly CA, Riley S, et al. Report 3: transmissibility of 2019-nCoV. Imperial College London; 2020. http://dx.doi.org/10.25561/77148.

# SUPPLEMENTARY MATERIAL

## Initial Infections

We defined the 169 infected workers at the Xinfadi Wholesale Market as initial infections. For each initial infection $i$, the time of infection $t_i^{inf}$ was either generated by subtracting a randomly sampled incubation period from the reported time of symptom onset (for a symptomatic case) or by subtracting a randomly sampled time delay from infection to diagnosis from the time of laboratory confirmation (for an asymptomatic case). The sampled time of infection was constrained within the exposure window identified by epidemiological investigation.

## SARS-CoV-2 Transmission as Branching Processes

We first generated each initial infection $i$'s reproduction number $R_i$ (number of secondary infections caused by $i$). For unmitigated transmission, we assumed that $R_i$ followed a negative binomial distribution $NB(R_0, k)$, where $R_0$ is the basic reproduction number representing the population average of $R_i$ and $k$ is the dispersion parameter capturing the heterogeneity of SARS-CoV-2 transmission. For each secondary infection $j \in \{R_i\}$, the infection time $t_j^{inf}$ is given by $t_j^{inf} = t_i^{inf} + \tau_{ij}$, where $\tau_{ij}$ denotes the generation interval of transmission from $i$ to $j$, drawn from a generation interval distribution $P_{GI}(\tau)$. Then, we hypothesized that the proportion of asymptomatic infection $\Phi_{asymp}$ decreased with age. For a symptomatic case $j$, we assigned his or her symptom onset date $t_j^{sym}$ by drawing from the incubation period distribution $P_{incu}(\tau)$. The parameters reflecting the transmission dynamics and the natural history of COVID-19 are summarized in Supplementary Table S1.

## Population Structure Reflecting Demographics, Transmission Setting, and Activity

When transmission between primary infection $i$ and secondary infection $j$ occurred, we first generated the transmission setting based on the predefined probability that the transmission event occurred at home ($\varnothing_{hh}$), in the workplace ($\varnothing_{wk}$) or in the community ($\varnothing_{cm}$). The hypothesized conditional probabilities are summarized in Supplementary Table S2, where we assumed that i) all service workers worked in the community and ii) all general workers did not work on holidays or weekends. For any transmission event occurring in the community, the activities of primary infection $i$ ($\mathrm{Act}_i$) and secondary infection $j$ ($\mathrm{Act}_j$) at the time of transmission were assigned based on their occupation. Service workers who worked in the community could be assigned either work or social activity, with probabilities of $\phi_{cm}^{wk}$=0.6 and $\phi_{cm}^{soc}$=0.4, respectively. For general workers and nonworkers, we assumed that only social activity was possible in the community (i.e., $\phi_{cm}^{wk} = 0$).

The age of secondary infection $j$ was then assigned based on transmission settings, age-stratified contact matrices and age-specific susceptibility to SARS-CoV-2 infection. We defined the age-specific contact matrices [derived from a prior study (*6*) and contact tracing data] as $C^{hh}$, $C^{wk}$, and $C^{cm}$ for household, workplace, and community contact, respectively. Each cell of the matrix ($c_{mk}^T$) represents the average number of contacts in age group $k$ of an individual in age group $m$ in a given setting $T$. For any contact in age group $k$, whether he or she became infected depended on the age-specific susceptibility to SARS-CoV-2 infection $risk_k^{inf}$ (derived from contact tracing data, Supplementary Table S3). Therefore, the probability that $j$ is in age group $a_j$ is given by

SUPPLEMENTARY TABLE S1. Parameters reflecting the transmission dynamics and the natural history of COVID-19.

| Parameter | Description | Value |
|---|---|---|
| $R_0$ | Basic reproduction number | 2.5 (*1*) |
| $k$ | Dispersion parameter capturing the heterogeneity of SARS-CoV-2 transmission | 0.43 (*2*) |
| $P_{GI}(\tau)$ | Distribution of generation interval | Gamma distribution (shape=13.86, rate=2.07) (*3*) |
| $\Phi_{asymp}$ | Age-specific asymptomatic rate | 46.7% for 0–18 years<br>32.1% for 19–59 years<br>19.7% for 60+ years (*4*) |
| $P_{incu}(\tau)$ | Distribution of the incubation period | Gamma distribution (derived from the epidemiological data) (shape=2.25, rate=0.39) |

Abbreviation: COVID-19=coronavirus disease 2019; SARS-CoV-2=severe acute respiratory syndrome coronavirus 2.

SUPPLEMENTARY TABLE S2. Hypothetical probability that the transmission event occurred at home, in the workplace or in the community.

| Condition | | Hypothetical probability | | |
|---|---|---|---|---|
| Occupation of primary infection $i$ ($O_i$) | Time of transmission ($t_j^{inf}$) | $\varnothing_{hh}$ | $\varnothing_{wk}$ | $\varnothing_{cm}$ |
| $hh\_suscept_i^*$ = 0 | | | | |
| General worker | Workday | 0 | 0.6 | 0.4 |
| | Holiday/weekend | 0 | 0 | 1 |
| Service worker | – | 0 | 0 | 1 |
| Nonworker | – | 0 | 0 | 1 |
| $hh\_suscept_i^*$ > 0 | | | | |
| General worker | Workday | 0.5 | 0.3 | 0.2 |
| | Holiday/weekend | 0.7 | 0 | 0.3 |
| Service worker | – | 0.5 | 0 | 0.5 |
| Nonworker | – | 0.7 | 0 | 0.3 |

Note: "–" means not applicable.
* $hh\_suscept_i$ denotes the number of susceptible individuals in primary infection $i$'s home at the time of transmission.

SUPPLEMENTARY TABLE S3. Age-specific susceptibility to SARS-CoV-2 infection.

| Age group ($k$) | Relative risk ($risk_k^{inf}$) |
|---|---|
| 0–14 years | 0.25 |
| 15–29 years | 0.79 |
| 30–49 years | 1 |
| 50–64 years | 1.13 |
| 65+ years | 1.32 |

$$P^T_{a_j|a_i} = \frac{c^T_{a_i a_j} risk^{inf}_{a_j}}{\sum_k C^T_{a_i k} risk^{inf}_k}$$

where $a_i$ is the age group of primary infection $i$. The sex of secondary infections was generated completely at random, except for individuals infected in the workplace aged 55–59 years (who were males because females retire from work at 55 years of age).

To assign secondary infection $j$'s occupation, we first determined whether he or she was a worker (i.e., 18–59 years for a male; 18–54 years for a female) according to his or her age and sex. We then divided workers into general workers (GW) and service workers (SW). Service workers were further divided into workers at the Xinfadi Wholesale Market (XFD-SW) and other service workers (Other-SW). For any infected worker $j$, we stochastically determined his or her specific occupation based on the predefined probability that the secondary infection $j$ worked as a general worker ($\psi_j^{GW}$), a service worker at the Xinfadi Wholesale Market ($\psi_j^{XFD-SW}$) or a service worker in other places ($\psi_j^{Other-SW}$). The hypothetical probabilities conditional on the transmission setting ($T_{ij}$), activity ($Act_i$) and occupation ($O_i$) of primary infection $i$ are summarized in Supplementary Table S4.

## Population Interaction Network Based on Spatially Resolved Mobility Patterns

To emulate the spatial dispersion of SARS-CoV-2 infections, we first constructed the spatially resolved population mobility patterns in Beijing on the basis of the mobility data and then developed a network interaction model based on the constructed mobility patterns to stochastically assign the residential locations of each person with an infection, the workplace of each worker and the location for social activity if the transmission occurred through social contact. Details are described below.

**Mobility data:** The aggregated mobile phone signaling data were provided by China Unicom, one of the leading mobile phone service providers in China. The data were aggregated as origin-destination matrices (O-D matrices)

SUPPLEMENTARY TABLE S4. Hypothetical probability that the secondary infection $j$ worked as a general worker, a service worker at the Xinfadi Wholesale Market or a service worker in other places.

| Condition | | Hypothetical probability* | | |
|---|---|---|---|---|
| $T_{ij}$ | $Act_i$ | $\psi_j^{GW}$ | $\psi_j^{XFD\text{-}SW}$ | $\psi_j^{Other\text{-}SW}$ |
| $O_i$=GW | | | | |
| At home | – | 0.903 | 0 | 0.097 |
| In the workplace | – | 1 | 0 | 0 |
| In the community | Social activity | 0.903 | 0 | 0.097 |
| $O_i$=XFD-SW | | | | |
| At home | – | 0.72 | 0.2 | 0.08 |
| In the community | Work | 0.4 | 0.2 | 0.4 |
| In the community | Social activity | 0.72 | 0.2 | 0.08 |
| $O_i$=Other-SW | | | | |
| At home | – | 0.903 | 0 | 0.097 |
| In the community | Work | 0.8 | 0 | 0.2 |
| In the community | Social activity | 0.903 | 0 | 0.097 |
| $O_i$=Nonworker | | | | |
| At home | – | 0.903 | 0 | 0.097 |
| In the community | Social activity | 0.903 | 0 | 0.097 |

Note: "–" means not applicable.
Abbreviation: GW=general worker; XFD-SW=service worker at the Xinfadi Market; Other-SW=service worker in other places.
* The probabilities are hypothesized based on epidemiological investigations of the outbreak and the demographical structures in Beijing (7).

stratified by age and sex group, where the rows and the columns represent the origin and destination streets/towns, respectively. Each cell of the matrix represents the total number of trips of the subscribers from the origin to the destination in a given age and sex group during a certain period of time (in hours).

**Spatially resolved mobility patterns in Beijing:** By aggregating the mobility data, we obtained the average number of trips from the origin location $O$ to the destination location $D$ at time $t$ in a given age and sex group on workday $n_{O\to D}^{wkd}(t|\, age, sex)$ and on holiday $n_{O\to D}^{hld}(t|\, age, sex)$, respectively. Assuming that the working-age population goes to work during morning rush hours (i.e., between 6:00 a.m. and 10:00 a.m. on workdays), we estimated the average daily trips from location $O$ to location $D$ for work ($n_{O\to D}^{work}$) as $n_{O\to D}^{work} = \sum_{t=6}^{10} n_{O\to D}^{wkd}(t|\, wk\_age)$, where $wk\_age$ refers to working age groups (i.e., 18–59 years for males and 18–54 years for females). Since service workers provide social services to the general population, we assumed that their spatial mobility patterns for work were in accordance with and accounted for 10% of the population flows on holiday morning rush hours. Therefore, the average number of daily trips of the service workers from $O$ to $D$ for work $n_{O\to D}^{sw}$ is given by $n_{O\to D}^{sw} = 0.1 \times \sum_{t=6}^{10} n_{O\to D}^{hld}(t|\, wk\_age)$, and that of the general workers $n_{O\to D}^{gw}$ can be derived as $n_{O\to D}^{gw} = n_{O\to D}^{work} - n_{O\to D}^{sw}$. Trips at other times or of other age groups were considered as social activities. Assuming that those who live in location $D$ and work at location $O$ would travel from $D$ to $O$ in the morning and back from $O$ to $D$ in the evening, the average daily trips from $O$ to $D$ for social activities are given as $n_{O\to D}^{soc\_wkd} = \sum_t n_{O\to D}^{wkd}(t|\, all) - n_{O\to D}^{work} - n_{D\to O}^{work}$ (on workday) and $n_{O\to D}^{soc\_hld} = \sum_t n_{O\to D}^{hld}(t|\, all) - n_{O\to D}^{sw} - n_{D\to O}^{sw}$ (on holiday), where $all$ refers to all age and sex groups.

Then, the interaction matrices reflecting the population mobility patterns in Beijing in the absence of non-pharmaceutical interventions were constructed based on the aggregated data before the Xinfadi outbreak (from June 1 to June 12, 2020), with each row of the matrices representing the origin street/town (i.e., residential location) and each column representing the destination street/town (i.e., location for work or social activity). Specifically, the interaction matrices for work are defined as $I^{gw}$ (for general workers) and $I^{sw}$ (for service workers), of which each cell represents the probability of working at location $D$ for an individual living in location $O$, given as $I_{O\to D}^{gw} = \frac{n_{O\to D}^{gw}}{\sum_K n_{O\to K}^{gw}}$ and $I_{O\to D}^{sw} = \frac{n_{O\to D}^{sw}}{\sum_K n_{O\to K}^{sw}}$. Similarly, the interaction matrices reflecting the social mobility patterns on workday ($I^{soc\_wkd}$)

and on holiday ($I^{soc\_hld}$) are constructed as $I^{soc\_wkd}_{O\to D} = \frac{n^{soc\_wkd}_{O\to D}}{\sum_K n^{soc\_wkd}_{O\to K}}$ and $I^{soc\_hld}_{O\to D} = \frac{n^{soc\_hld}_{O\to D}}{\sum_K n^{soc\_hld}_{O\to K}}$, respectively.

**Network interaction model:** Locations of secondary infections were stochastically allocated using a spatially structured network interaction model based on the constructed mobility patterns. We first created a unique block identification number $blk\_id$ for each residential block and a unique household identification number $hh\_id$ for each family, where residents of a block share the same $blk\_id$ and members of a household share the same $hh\_id$.

Household transmission: For any transmission occurred at home,the residential location and household size of the secondary infection $j$ were the same as those of the primary infector $i$, i.e., $loc\_resid_j = loc\_resid_i$, $blk\_id_j = blk\_id_i$, $hh\_id_j = hh\_id_i$, $hh\_size_j = hh\_size_i$. The workplace of $j$ ($loc\_wk_j$) is then chosen based on the mobility patterns, given as $P_{(loc\_wk_j=D)} = I^{gw}_{loc\_resid_j\to D}$ (if $j$ is a general worker) or $P_{(loc\_wk_j=D)} = I^{sw}_{loc\_resid_j\to D}$ (if $j$ is a service worker), where $P_{(loc\_wk_j=D)}$ indicates the probability that $j$ worked at location $D$.

Workplace transmission: If a transmission event occurred in the workplace, we have $loc\_wk_j = loc\_wk_i$. The residential street/town of the secondary infection $j$ was then allocated according to the mobility patterns, given as $P_{(loc\_resid_j=O)} = I^{gw}_{O\to loc\_wk_j}$. We further randomly chose a $blk\_id$ and a $hh\_id$ for $j$ within his or her residential street/town and stochastically generated $j$'s household size based on the age-specific household size distribution (*6*).

Community transmission: For any transmission that occurred in the community, we first allocated a transmission location ($loc^{trans}_{i\to j}$). If $i$ infected $j$ through work contact (i.e., $\mathrm{Act}_i = work$), we have $loc^{trans}_{i\to j} = loc\_wk_i$. Otherwise, if $i$ infected $j$ through social contact (i.e., $\mathrm{Act}_i = social$), $loc^{trans}_{i\to j}$is stochastically generated following the probabilities given as $P_{(loc^{trans}_{i\to j}=D)} = I^{soc\_wkd}_{loc\_resid_i\to D}$ (on a workday) or $P_{(loc^{trans}_{i\to j}=D)} = I^{soc\_hld}_{loc\_resid_i\to D}$ (on a holiday). Then, $j$'s residential street/town and workplace are generated according to $\mathrm{Act}_j$ and $loc^{trans}_{i\to j}$: (i) if $j$ was infected through work contact (i.e., $\mathrm{Act}_j = work$), we have $loc\_wk_j = loc^{trans}_{i\to j}$. The residential location of $j$ is randomly generated following the probability $P_{(loc\_resid_j=O)} = I^{sw}_{O\to loc\_wk_j}$. (ii) If $j$ was infected through social contact (i.e., $\mathrm{Act}_j = social$), we first randomly assigned $j$'s residential location based on the population mobility patterns, given as $P_{(loc\_resid_j=O)} = I^{soc\_wkd}_{O\to loc^{trans}_{i\to j}}$ (on workday) and $P_{(loc\_resid_j=O)} = I^{soc\_hld}_{O\to loc^{trans}_{i\to j}}$ (on holiday). The workplace of $j$ ($loc\_wk_j$) is then chosen according to his or her occupation, given as $P_{(loc\_wk_j=D)} = I^{gw}_{loc\_resid_j\to D}$ (if $j$ is a general worker) or $P_{(loc\_wk_j=D)} = I^{sw}_{loc\_resid_j\to D}$ (if $j$ is a service worker). Finally, we randomly chose a $blk\_id$ and a $hh\_id$ for $j$ within his or her residential street/town and stochastically generated $j$'s household size based on the age-specific household size distribution (*6*).

## Non-Pharmaceutical Interventions (NPIs)

**Symptomatic surveillance:** Initially, we assumed that 33.3% of the people with symptomatic infections (i.e., $\Phi_{hosp}$ = 33.3%) would seek medical attention after a mean time delay of 3.7 days from the onset of symptoms. After the official report of the outbreak on June 13, 2020, with enhanced symptom surveillance in the community, we assumed that more people with symptomatic infections (i.e., $\Phi_{hosp}$ = 66.7%) would seek health care consultation after a shorter time delay with a mean of 2.7 days from symptom onset. Three RT-PCR (i.e., reverse transcription polymerase chain reaction) tests for SARS-CoV-2 diagnosis were conducted on the 1st, 3rd and 7th days of isolation. The sensitivity of RT-PCR testing was assumed to vary with time, following the estimates of a prior study (*8*).

**Mask wearing:** We assume 20% of the population would wear masks in the workplace and 50% in the community. The protective effect of mask wearing against further transmission and infection of SARS-CoV-2 was assumed to be 9.5% and 18%, respectively (*9*–*10*).

**Closure of the Xinfadi Wholesale Market:** The Xinfadi Wholesale Market was closed on June 13, 2020.

**Quarantine and testing of key populations:** Workers at the Xinfadi Wholesale Market were quarantined in centralized facilities for at least 14 days. Periodic RT-PCR testing was conducted on the 1st, 4th, 7th, and 14th days of quarantine and the 2nd and 7th days after discharge. Visitors who had been to the Xinfadi Wholesale Market between May 30 and June 12, 2020, were asked to stay at home for 14 days. RT-PCR testing was performed on the 1st, 7th and 14th days of home quarantine. Residents living around the Xinfadi Wholesale Market were confined to their living communities from June 13, 2020, until no new infections were reported for 14 consecutive days. Mass testing was implemented every seven days during the lockdown period.

**Contact tracing:** Close contact was defined as a person who interacted with a confirmed case from 4 days before to 14 days after illness onset or with an asymptomatic carrier from 4 days before to 14 days after collection of the first positive sample. We assumed that all household contacts were immediately quarantined, while all work contacts and 70% of the community contacts quarantined with a mean time delay of 3 days. Centralized quarantine at designated facilities for at least 14 days was required for all close contacts, with periodic RT-PCR testing on the 1st, 4th, 7th, and 14th days of quarantine and the 2nd and 7th days after discharge.

**Residential community lockdown:** Since June 13, 2020, residential communities with detected infections have been on lockdown at the block level until 14 days after the identification of the last case, with stay-at-home orders for all residents other than essential workers.

**Mobility restrictions:** During the Xinfadi outbreak, the street/town was upgraded to moderate risk once it had reported more than one infection and then upgraded to high risk when more than 5 infections were reported, while other regions, with or without one detected infection, remained low-risk areas. We quantified the reduction in population flows and constructed the origin-destination mobility matrix between different risk regions based on mobility data (Supplementary Table S5).

SUPPLEMENTARY TABLE S5. The hypothetical origin-destination mobility matrix depending on risk levels.

| Risk level of the origin street/town | Risk level of the destination street/town | | | Mobility within one street/town |
|---|---|---|---|---|
| | High | Moderate | Low | |
| High | 0 | 0.1 | 0.3 | 0.3 |
| Moderate | 0.1 | 0.3 | 0.5 | 0.6 |
| Low | 0.3 | 0.5 | 0.8 | 0.9 |

Note: The risk level refers to the real-time risk level of the street/town at the time of transmission. The value in each cell of the matrix refers to the average travel probability per person after the Xinfadi outbreak, given the risk level of the origin and destination regions.

**Mass testing:** Three rounds of RT-PCR testing were required for all residents living in streets/towns with detected infections, with each round of mass testing being completed within 3–4 days. The interval between each round of testing was usually 7 days.

## REFERENCES


1. Imai N, Cori A, Dorigatti I, Baguelin M, Donnelly CA, Riley S, et al. Report 3: transmissibility of 2019-nCoV. Imperial College London; 2020. http://dx.doi.org/10.25561/77148.
2. Adam DC, Wu P, Wong JY, Lau EHY, Tsang TK, Cauchemez S, et al. Clustering and superspreading potential of SARS-CoV-2 infections in Hong Kong. Nat Med 2020;26(11):1714 – 9. http://dx.doi.org/10.1038/s41591-020-1092-0.
3. Zhao S, Tang B, Musa SS, Ma SJ, Zhang JY, Zeng MY, et al. Estimating the generation interval and inferring the latent period of COVID-19 from the contact tracing data. Epidemics 2021;36:100482. http://dx.doi.org/10.1016/j.epidem.2021.100482.
4. Sah P, Fitzpatrick MC, Zimmer CF, Abdollahi E, Juden-Kelly L, Moghadas SM, et al. Asymptomatic SARS-CoV-2 infection: a systematic review and meta-analysis. Proc Natl Acad Sci USA 2021;118(34):e2109229118. http://dx.doi.org/10.1073/pnas.2109229118.
5. Zhang JJ, Klepac P, Read JM, Rosello A, Wang XL, Lai SJ, et al. Patterns of human social contact and contact with animals in Shanghai, China. Sci Rep 2019;9(1):15141. http://dx.doi.org/10.1038/s41598-019-51609-8.
6. Beijing Municipal Bureau of Statistics, Survey Office of the National Bureau of Statistics in Beijing. Annual statistics of population and employment in Beijing in 2021. 2020. http://tjj.beijing.gov.cn/tjsj_31433/tjbmfbjh/ndtjzl_31437/2021ndtjzl/202012/t20201231_2191210.html. [2022-8-6]. (In Chinese).
7. Kucirka LM, Lauer SA, Laeyendecker O, Boon D, Lessler J. Variation in false-negative rate of reverse transcriptase polymerase chain reaction-based SARS-CoV-2 tests by time since exposure. Ann Intern Med 2020;173(4):262 – 7. http://dx.doi.org/10.7326/m20-1495.
8. Bundgaard H, Bundgaard JS, Raaschou-Pedersen DET, von Buchwald C, Todsen T, Norsk JB, et al. Effectiveness of adding a mask recommendation to other public health measures to prevent SARS-CoV-2 infection in danish mask wearers: a randomized controlled trial. Ann Intern Med 2021;174(3):335 – 43. http://dx.doi.org/10.7326/m20-6817.
9. Leech G, Rogers-Smith C, Sandbrink JB, Snodin B, Zinkov R, Rader B, et al. Mass mask-wearing notably reduces COVID-19 transmission. medRxiv 2021. http://dx.doi.org/10.1101/2021.06.16.21258817.